Journal of Sound and Vibration (2002) **251**(3), 409–430
doi:10.1006/jsvi.2001.4007, available online at http://www.idealibrary.com on IDEAL®

PREDICTION AND MEASUREMENT OF SOME DYNAMIC PROPERTIES OF SANDWICH STRUCTURES WITH HONEYCOMB AND FOAM CORES

E. NILSSON AND A. C. NILSSON

The Marcus Wallenberg Laboratory for Sound and Vibration Research (MWL), Department of Vehicle Engineering, KTH, SE-100 44 Stockholm, Sweden.
E-mail: andersni@fkt.kth.se

(*Received* 4 *April* 2001, *and in final form* 21 *August* 2001)

Some dynamical properties of sandwich beams and plates are discussed. The types of elements investigated are three-layered structures with lightweight honeycomb or foam cores with thin laminates bonded to each side of the core. A six order differential equation governing the apparent bending of sandwich beams is derived using Hamilton's principle. Bending, shear and rotation are considered. Boundary conditions for free, clamped and simply supported beams are formulated. The apparent bending stiffness of sandwich beams is found to depend on the frequency and the boundary conditions for the structure. Simple measurements on sandwich beams are used to determine the bending stiffness of the entire structure and at the same time the bending stiffness of the laminates as well as the shear stiffness of the core. A method for the prediction of eigenfrequencies and modes of vibration are presented. Eigenfrequencies for rectangular and orthotropic sandwich plates are calculated using the Rayleigh–Ritz technique assuming frequency dependent material parameters. Predicted and measured results are compared.

1. INTRODUCTION

The number of applications for sandwich structures is steadily increasing. This trend is dictated by demands for higher load capacity for civil and military aircraft, reduced fuel consumption for passenger cars, increased speed for passenger and navy vessels of catamaran types and increased acceleration and retardation for trains to increase the average velocity. The term sandwich panel here refers to a structure consisting of two thin faces bonded to a thick and lightweight core. The faces are typically of aluminium or some composite laminate. The core could be lightweight foam or a honeycomb structure. There are a large number of papers and publications on the dynamic properties of sandwich structures. Already in 1950, Hoff [1] concluded that there was an abundance of theoretical work in the field. Some of the basic theories are now also summarized in textbooks. Two examples are references [2, 3].

The bending of sandwich beams and plates is often described by means of some simplified model. Often a variational technique is used to derive the basic equations governing the vibrations of sandwich structures. The Timoshenko [4] and Mindlin [5] models are frequently referred to. Various types of finite element models are alternative methods. One of the first fundamental works on the bending and buckling of sandwich plates was published by Hoff [1]. In this paper, Hamilton's principle is used to derive the differential

0022-460X/02/130409 + 22 $35.00/0

equations governing the bending and buckling of rectangular sandwich panels subjected to transverse loads and edgewise compression. The basic ideas introduced by Hoff form the basis for many subsequent papers on the bending of sandwich plates.

Another by now classic paper was published by Kurtze and Watters [6] in 1959. The aim of the paper was to develop a simple model to predict the sound transmission through sandwich panels. The starting point was a model describing the bending of the panel based on the mechanical impedance of each layer. The laminates are described as thin plates. The thick core is isotropic and only shear effects are included. The bending stiffness of the plate is found to vary between two limits; the high-frequency asymptote is determined by the bending stiffness of the laminates. The model was later somewhat improved by Dym and Lang [7]. Boundary conditions are not discussed in references [6, 7].

A more general description of the bending of sandwich beams is given by Nilsson [8]. In this model, the laminates are again described as thin plates. However, the general wave equation is used to describe the displacement in the core. The influence of boundary conditions is not discussed. The model is used to predict the sound transmission loss of sandwich plates. Some boundary conditions and their influence on the bending stiffness of a structure were later discussed by Sander [9] using the model presented in reference [8].

Guyader and Lesueur [10] investigated the sound transmission through multilayered orthotropic plates. The description of the displacement of each layer is based on a model suggested by Sun and Whitney [11]. A certain computational effort is required. Renji *et al.* derive a simple differential equation governing the apparent bending of sandwich panels in reference [12]. The model includes shear effects. Compared to measured results, the shear effects were overestimated. In particular, in the high-frequency region the predicted bending stiffness is too low. A modified Mindlin plate theory is suggested by Liew [13]. The influence of some boundary conditions is also discussed in a subsequent paper [14]. Again, a certain computational effort is required. Maheri and Adams [15] used the Timoshenko beam equations to describe flexural vibrations of sandwich structures. In particular, effects of variations of the shear coefficient are discussed for obtaining satisfactory results.

Common to many of these references is the fact that the governing differential equations derived are of the fourth order. Due to the frequency dependence of sandwich structures, the solutions with four unknowns will agree very well for low frequencies. On the other hand, as frequency increases the calculated result will disagree strongly with measurements.

The main work on sandwich construction relates to conventional foam-core structures with various facings. Little work has been done on the dynamics of honeycomb panels. In 1997, Saito *et al.* [16] proposed a method on how to identify the dynamic parameters for aluminium honeycomb panels using orthotropic Timoshenko beam theory. They used a second order differential equation and determined the dynamic parameters by comparing their theories with frequency response measurements. Chao and Chern [17] proposed a three dimensional (3-D) theory for the calculation of the eigenfrequencies of laminated rectangular plates. The paper also includes a useful reference list, each reference being classified according to the method used.

Various finite element methods are often proposed for describing the vibration of sandwich panels. For example, a finite element vibration analysis of composite beams based on Hamilton's principle is presented by Shi and Lam [18]. A standard FEM code is used by Cummingham *et al.* [19] to determine the eigenfrequencies of curved sandwich panels. The agreement between predicted and measured eigenfrequencies is found to be very good. Liew *et al.* [20] used a finite element model for the numerical evaluation of frequency response functions of honeycomb panels. Structures with and without delamination were considered. In the study, the honeycomb structure was modelled as a three-layer substructure with the use of a 3-D solid polyhedron element.

There are a large number of methods describing the vibration of sandwich panels. However, the aim of this work is to formulate simple but sufficiently accurate equations governing the apparent bending of sandwich beams and plates. Boundary conditions should also be formulated for the calculation of eigenfrequencies and modes of vibration. The models should allow simple parameter studies for the optimization of the structures with respect to their acoustic performance. The aim is also to describe a simple measurement technique for determining some of the material parameters of composite beams.

2. HONEYCOMB PANELS

A honeycomb panel is a thin lightweight plate with a honeycomb core with hexagonal cells. Layered laminates are bonded to both sides of the core as shown in Figure 1. Each component is by itself relatively weak and flexible. When combined into a sandwich panel the elements form a stiff, strong and lightweight structure. The facings carry the bending loads and the core carries the shear loads. In general, the honeycomb core is strongly orthotropic.

The types of core materials in the panels used for the measurements presented here are Nomex or aluminium. Nomex is an aramid fibre paper dipped in phenolic resin with low shear modulus and shear strength. A typical thickness of the Nomex honeycomb panels investigated is 10 mm with the thickness of the laminate being between 0·3–0·7 mm. The weight per unit area is of the order of 3 kg/m^2/unit area. Each laminate consists of 3–5 different layers bonded together to give the best possible strength. The laminates are not necessarily symmetric and are usually orthotropic. The core acts as a spacer between the two laminates to give the required bending stiffness for the entire beam. The bending stiffness of the core itself is in general very low.

The cells in the core give an orthotropic structure. The dynamic characteristics should be expected to vary in all directions. The shape of the honeycomb cells of a typical aluminium core is generally very irregular which makes it impossible to describe its geometry in a simple way. Nomex cores have very regular shapes as compared to Al-cores.

The normal deflection of a honeycomb panel is primarily caused not only by bending but also by shear and rotation in the core. A honeycomb panel could be compared to a three-layered panel as seen in Figure 2. The figure shows (1) the deflection of a beam due to pure bending and (2) due to shear in the core.

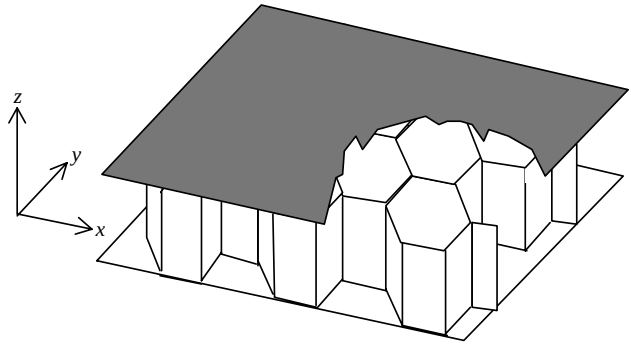

Figure 1. Sandwich panel with a honeycomb core.

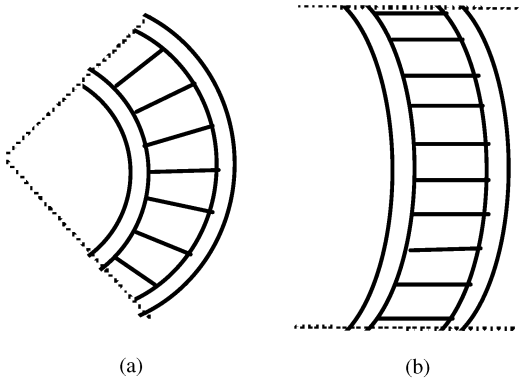

Figure 2. Deflection caused by bending (a) and shear (b).

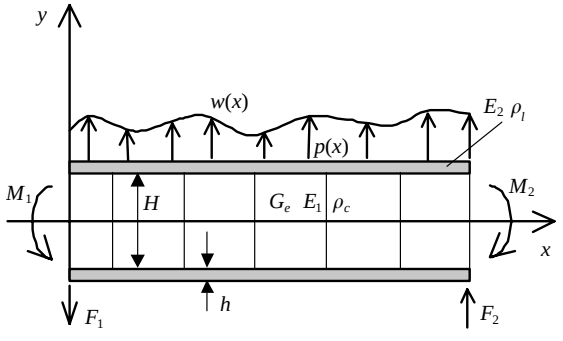

Figure 3. Excitation of a beam and resulting forces and moments. Dimensions and material parameters for laminates and core are indicated.

3. FLEXURAL VIBRATION OF SANDWICH BEAMS

The total lateral displacement w of a sandwich beam is a result of the angular displacement due to bending of the core as defined by β and the angular displacement due to shear in the core γ as

$$\frac{\partial w}{\partial x} = \gamma + \beta. \tag{1}$$

The differential equations governing w, β and γ can be determined using Hamilton's principle [4], which for a conservative system is formulated as

$$\delta \int\int (U - T + A)\,\mathrm{d}x\,\mathrm{d}t = 0, \tag{2}$$

where U is the potential energy per unit length and T the corresponding kinetic energy per unit length and A the potential energy induced per unit length by external and conservative forces. The energies U and T are derived as functions of the displacement of the beam.

In deriving the equations governing the lateral displacement of the structure shown in Figure 3, symmetry is assumed. The identical laminates have a Young's modulus E_2,

bending stiffness D_2, density ρ_l and thickness h. The effective shear stiffness of the core is G_e, its Young's modulus E_1, its equivalent density ρ_c and its thickness H. The parameter G_e is for a thick core not necessarily equal to the shear stiffness G as suggested by Timoshenko [21]. The core itself is assumed to have a very low stiffness in the x-direction. In the y-direction, the core is assumed to be sufficiently stiff to ensure that the laminates move in phase within the frequency range of interest.

The bending stiffness per unit width of the beam is

$$D_1 = E_1 H^3/12 + E_2(H^2 h/2 + Hh^2 + 2h^3/3). \tag{3}$$

In general, $E_2 \gg E_1$. The bending stiffness of one laminate is

$$D_2 = E_2 h^3/12. \tag{4}$$

The mass moment of inertia per unit width is defined as

$$I_\rho = \rho_c H^3/12 + \rho_l(H^2 h/2 + Hh^2 + 2h^3/3) \tag{5}$$

while the mass per unit area is

$$\mu = 2h\rho_l + H\rho_c. \tag{6}$$

According to Hamilton's principle, equation (2), the kinetic and potential energies of the structure must be defined as functions of the displacement of the beam defined by w, β and γ as in equation (1). The total potential energy of a honeycomb beam is due to pure bending of the entire beam, bending of both laminates and shear in the core. The total potential energy of a beam, width b and length L, is thus

$$U = \frac{b}{2}\int_0^L \left(D_1\left(\frac{\partial\beta}{\partial x}\right)^2 + 2D_2\left(\frac{\partial\gamma}{\partial x}\right)^2 + G_e H\gamma^2 \right) \mathrm{d}x. \tag{7}$$

The kinetic energy of the honeycomb panel consists of two parts, the kinetic energy due to vertical motion of the beam and the kinetic energy due to the rotation of a section of the beam. This gives the total kinetic energy of the beam as

$$T = \frac{b}{2}\int_0^L \left(\mu\left(\frac{\partial w}{\partial t}\right)^2 + I_\rho\left(\frac{\partial\beta}{\partial t}\right)^2 \right) \mathrm{d}x. \tag{8}$$

The total potential energy for the conservative external forces according to Figure 3 is

$$\begin{aligned} -A &= b\int_0^L pw\,\mathrm{d}x + b[F_2 w(L) - F_1 w(0) - M_2\beta(L) + M_1\beta(0)] \\ &= b\int_0^L pw\,\mathrm{d}x + b[Fw - M\beta]_0^L, \end{aligned} \tag{9}$$

where F is the force per unit width, M the moment per unit width and p the external pressure on the beam. The moments and forces are defined in Figure 3. By using the definition of γ, equation (1), and by inserting equations (7)–(9) into the variational

expression (2) the result is

$$\delta\iint\left\{D_1\left(\frac{\partial\beta}{\partial x}\right)^2+2D_2\left(\frac{\partial^2 w}{\partial x^2}-\frac{\partial\beta}{\partial x}\right)^2+G_eH\left(\frac{\partial w}{\partial x}-\beta\right)^2-\mu\left(\frac{\partial w}{\partial t}\right)^2-I_\rho\left(\frac{\partial\beta}{\partial t}\right)^2\right\}\frac{\mathrm{d}x\,\mathrm{d}t}{2}$$

$$-\delta\iint pw\,\mathrm{d}x\,\mathrm{d}t-\delta\int[Fw-M\beta]_0^L\,\mathrm{d}t=0. \tag{10}$$

The integration over time is from t_0 to t_1 and over the length from 0 to L. Effecting the variation as demonstrated in reference [22], it is found that the displacement w and the angular displacement β must satisfy the differential equations

$$-G_eH\left(\frac{\partial^2 w}{\partial x^2}-\frac{\partial\beta}{\partial x}\right)+2D_2\left(\frac{\partial^4 w}{\partial x^4}-\frac{\partial^3\beta}{\partial x^3}\right)+\mu\frac{\partial^2 w}{\partial t^2}-p=0, \tag{11}$$

$$-D_1\frac{\partial^2\beta}{\partial x^2}+2D_2\left(\frac{\partial^3 w}{\partial x^3}-\frac{\partial^2\beta}{\partial x^2}\right)+I_\rho\frac{\partial^2\beta}{\partial t^2}-G_eH\left(\frac{\partial w}{\partial x}-\beta\right)=0. \tag{12}$$

On eliminating β the equation governing w is obtained as

$$-2D_1D_2\frac{\partial^6 w}{\partial x^6}+2D_2I_\rho\frac{\partial^6 w}{\partial x^4\partial t^2}-(D_1\mu+2D_2\mu+I_\rho G_eH)\frac{\partial^4 w}{\partial x^2\partial t^2}+G_eH\left(D_1\frac{\partial^4 w}{\partial x^4}+\mu\frac{\partial^2 w}{\partial t^2}\right)$$

$$+I_\rho\mu\frac{\partial^4 w}{\partial t^4}=\frac{\partial^2 p}{\partial x^2}(D_1+2D_2)-G_eHp-I_\rho\frac{\partial^2 p}{\partial t^2}. \tag{13}$$

Elimination of w instead gives the corresponding equation for β as

$$-2D_1D_2\frac{\partial^6\beta}{\partial x^6}+2D_2I_\rho\frac{\partial^6\beta}{\partial x^4\partial t^2}-(D_1\mu+2D_2\mu+I_\rho G_eH)\frac{\partial^4\beta}{\partial x^2\partial t^2}+G_eH\left(D_1\frac{\partial^4\beta}{\partial x^4}+\mu\frac{\partial^2\beta}{\partial t^2}\right)$$

$$+I_\rho\mu\frac{\partial^4\beta}{\partial t^4}=-2D_2\frac{\partial^3 p}{\partial x^3}+G_eH\frac{\partial p}{\partial x}. \tag{14}$$

The shear angle γ can be shown to satisfy the same differential equation as β, equation (14). The boundary conditions to be satisfied are also obtained from the variational expression (10) as

$$F=G_eH\left(\frac{\partial w}{\partial x}-\beta\right)-2D_2\left(\frac{\partial^3 w}{\partial x^3}-\frac{\partial^2\beta}{\partial x^2}\right)\quad\text{or}\quad w=0, \tag{15}$$

$$M=-D_1\frac{\partial\beta}{\partial x}+2D_2\left(\frac{\partial^2 w}{\partial x^2}-\frac{\partial\beta}{\partial x}\right)\quad\text{or}\quad\beta=0, \tag{16}$$

$$0=\left(\frac{\partial^2 w}{\partial x^2}-\frac{\partial\beta}{\partial x}\right)\quad\text{or}\quad\frac{\partial w}{\partial x}=0. \tag{17}$$

These equations provide the boundary conditions for a beam. Using the wave equations (13) and (14) together with the six boundary conditions, three at each end, the displacements

w and β can be determined. For free vibrations, the external pressure p is equal to zero allowing w and β to satisfy the same differential equation.

4. BOUNDARY CONDITIONS

For a beam with clamped, free or so-called simply supported edges, the boundary conditions can be formulated based on results (15)–(17). For a clamped beam, the displacement as well as the angular displacement must equal zero at the boundary. From this it follows that $w = \partial w/\partial x = 0$ at the edge to satisfy equations (15) and (17). In addition, $M \neq 0$. Thus to satisfy equation (16) β must equal zero.

At a free edge $F$and M, given in equations (15) and (16), are zero. The rotation $\partial w/\partial x$ is different from zero. Consequently, the requirement defined in equation (17) is only satisfied if $\partial^2 w/\partial x^2 = \partial\beta/\partial x$. This condition in combination with the requirement $M = 0$ defines the boundary condition for a clamped edge as $\partial\beta/\partial x = 0$ and $\partial^2 w/\partial x^2 = 0$. However the requirement $F = 0$, where F is defined in equation (15), gives when inserted into equation (12) the final condition relating to a free edge as $D_1\partial^2\beta/\partial x^2 = I_\rho\partial^2\beta/\partial t^2$.

For simply supported boundary conditions, it is assumed that the beam is hinged at the centre line or rather the neutral axis of the beam. The displacement and the bending moment at this point are equal to zero. For $\beta \neq 0$ and $\partial w/\partial x \neq 0$, equations (16) and (17) give $\partial\beta/\partial x = 0$ and $\partial^2 w/\partial x^2 = 0$ at a simply supported edge. In summary, the boundary conditions are listed in Table 1.

5. WAVENUMBERS

By assuming a solution $w = \exp[\mathrm{i}(\omega t - k_x x)]$ to the wave equation (13) and allowing the external pressure p to equal zero, the wavenumber k_x must satisfy the expression

$$2D_2 k_x^6 - \frac{2D_2}{D_1} I_\rho k_x^4 \omega^2 - \left(\mu + \frac{2D_2}{D_1}\mu + \frac{I_\rho G_e H}{D_1}\right) k_x^2 \omega^2 + G_e H\left(k_x^4 - \frac{\mu}{D_1}\omega^2\right) + \frac{I_\rho \mu}{D_1}\omega^4 = 0. \tag{18}$$

The six solutions to this equation are written as $k_x = \pm\kappa_1, \pm\mathrm{i}\kappa_2$ and $\pm\mathrm{i}\kappa_3$ where κ_1 and κ_3 are real whereas κ_2 can shift from being real to imaginary for increasing frequencies. By defining the stiffnesses as $D_n = D_{0n}(1 + \mathrm{i}\eta_n)$ and $G_e = G_{0e}(1 + \mathrm{i}\eta_e)$ losses are included. The absolute values of the wavenumbers are shown in Figure 4. The material and geometrical parameters describing the beam, denoted as A_x, are given in Table 2. The lower of the two parallel lines in Figure 4 represents the wavenumber corresponding to pure

TABLE 1

Boundary conditions

Clamped end	$w = 0,$	$\beta = 0,$	$\dfrac{\partial w}{\partial x} = 0$
Simply supported end	$w = 0,$	$\dfrac{\partial\beta}{\partial x} = 0,$	$\dfrac{\partial^2 w}{\partial x^2} = 0$
Free end	$\dfrac{\partial^2 w}{\partial x^2} = 0,$	$\dfrac{\partial\beta}{\partial x} = 0,$	$D_1\dfrac{\partial^2\beta}{\partial x^2} = I_\rho\dfrac{\partial^2\beta}{\partial t^2}$

TABLE 2

Geometrical and material parameters for beams. $L = 1{\cdot}2$ m for all beams

Material	A_y Nomex h.c.	A_x Nomex h.c.	C_y Al h.c.	C_a Al h.c.	C_b Al h.c.	D foam core	E h.c.
b (m)	0·1	0·1	0·1	0·1	0·1	0·1	0·1
h (mm)	0·5	0·5	0·8	0·8	0·8	0·8	0·8
H (mm)	10	10	17·6	17·6	17·6	16·3	17·1
ρ_{lam} (kg/m^3)	1264	1264	2700	2700	2700	2700	2700
ρ_{core} (kg/m^3)	137·6	137·6	106·8	106·8	106·8	103·1	69·0
μ (kg/m^2)	2·64	2·64	6·2	6·2	6·2	6·0	5·5
G_e (MPa)	136	80	560	5600	5600	23	287
E_2 (GPa)	32	55	70	70	80	70	70

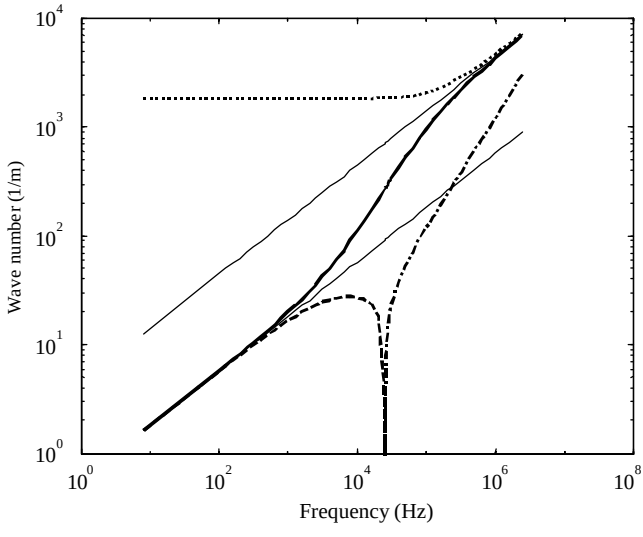

Figure 4. Wavenumbers for beam A_x. ——, κ_1; - - - -, κ_2 (evanescent); -·-·-·-, κ_2 (propagating); ·····, κ_3. The parallel lines are asymptotes for the wavenumber.

bending of the entire beam. The upper line represents the wavenumber for pure bending of one of the identical laminates. The parallel lines define the low- and high-frequency limits for the wavenumber κ_1 for the first propagating mode. In the mid-frequency region shear and rotation become important. As these effects increase, the wavenumber deviates from the lower asymptote and shifts towards the upper one.

The dotted and the dashed lines in Figure 4 represents the purely imaginary roots given by κ_2 and κ_3 and correspond to the nearfield solutions or the evanescent waves for the in-phase motion of the laminates. The constant value for low frequencies, the dotted line, is determined by the thickness of the core. For increasing frequencies, this curve approaches the limit determined by the wavenumber for evanescent waves in one of the identical laminates. Decreasing the thickness of the core will increase the constant value in the lowest frequency range. The other nearfield solution closely follows the asymptote for the bending of the entire beam for low frequencies. As the frequency increases, κ_2 approaches zero for

$f = f_p$ where

$$f_p = \frac{1}{2\pi}\sqrt{\frac{G_e H}{I_\rho}}. \tag{19}$$

For frequencies below f_p the wavenumber $k_x = \pm i\kappa_2$ is imaginary, defining evanescent waves. For higher frequencies, $k_x = \pm i\kappa_2$ is real representing a rotating and propagating wave. The frequency f_p is decreased as the moment of inertia is decreased and thus when the thickness H is increased. For beams with thick foam cores, the frequency f_p tends to be fairly low.

In summary, the limiting values for the wavenumbers are

$$\lim_{f\to 0}|\kappa_1| = \lim_{f\to 0}|\kappa_2| = \left[\frac{\mu\omega^2}{D_1}\right]^{1/4}, \quad \lim_{f\to 0}|\kappa_3| = \left[\frac{G_e H}{2D_2}\right]^{1/2},$$

$$\lim_{f\to \infty}|\kappa_1| = \lim_{f\to \infty}|\kappa_3| = \left[\frac{\mu\omega^2}{2D_2}\right]^{1/4}, \quad \lim_{f\to \infty}|\kappa_2| = \left[\frac{I_\rho\omega^2}{D_1}\right]^{1/2}. \tag{20}$$

6. DISPLACEMENT

For a honeycomb beam oriented along the x-axis, the displacement w and the angular displacement β must satisfy the differential equations (13) and (14). The displacement w must be defined as a function of the wavenumbers κ_1, κ_2 and κ_3. Consequently,

$$w = (A_1 \sin\kappa_1 x + A_2 \cos\kappa_1 x + A_3 e^{-\kappa_2 x} + A_4 e^{\kappa_2 (x-L)} + A_5 e^{-\kappa_3 x} + A_6 e^{\kappa_3 (x-L)})e^{i\omega t}, \tag{21}$$

where the amplitudes A_1–A_6 are determined by the boundary conditions and the external forces. The angular displacement β due to pure bending of the beam satisfies for $p = 0$ the same differential equation as w as given by equations (13) and (14). The angular displacement can therefore be expressed in a similar way as w. Thus,

$$\beta = (B_1 \sin\kappa_1 x + B_2 \cos\kappa_1 x + B_3 e^{-\kappa_2 x} + B_4 e^{\kappa_2 (x-L)} + B_5 e^{-\kappa_3 x} + B_6 e^{\kappa_3 (x-L)})e^{i\omega t}, \tag{22}$$

where κ_1, κ_2 and κ_3 are solutions to equation (18). In order to completely describe the displacement w and β for a beam, the parameters A_i and B_i need to be determined. However, the parameters A_i and B_i are not independent of each other. By inserting definitions (21) and (22) into equation (12), the result is found to be a function of $\sin\kappa_1 x$, $\cos\kappa_1 x$ etc. The total expression should be valid for any x. Thus it follows that the amplitudes of the functions $\sin\kappa_1 x$, $\cos\kappa_1 x$, etc. must equal zero. Consequently, the amplitudes B_i can be determined as functions of the amplitudes A_j. The result, using the abbreviations $D_t = D_1 + 2D_2$ and $\Omega = G_e H - \omega^2 I_\rho$, is

$$B_1 = -A_2 \frac{(2D_2\kappa_1^3 + G_e H\kappa_1)}{(D_t\kappa_1^2 + \Omega)} = A_2 X_2, \quad B_2 = A_1 \frac{(2D_2\kappa_1^3 + G_e H\kappa_1)}{(D_t\kappa_1^2 + \Omega)} = A_1 X_1,$$

$$B_3 = -A_3 \frac{(2D_2\kappa_2^3 - G_e H\kappa_2)}{(D_t\kappa_2^2 - \Omega)} = A_3 X_3, \quad B_4 = A_4 \frac{(2D_2\kappa_2^3 - G_e H\kappa_2)}{(D_t\kappa_2^2 - \Omega)} = A_4 X_4,$$

$$B_5 = -A_5 \frac{(2D_2\kappa_3^3 - G_e H\kappa_3)}{(D_t\kappa_3^2 - \Omega)} = A_5 X_5, \quad B_6 = A_6 \frac{(2D_2\kappa_3^3 - G_e H\kappa_3)}{(D_t\kappa_3^2 - \Omega)} = A_6 X_6. \tag{23}$$

From these results, it follows that $X_1 = -X_2$, $X_3 = -X_4$ and $X_5 = -X_6$. For a finite beam there are three boundary conditions at each end to be satisfied. These boundary conditions are sufficient for determining the relative amplitudes A_2/A_1, etc. as well as the eigenfrequencies for the beam.

The procedure for defining the eigenfrequencies and their corresponding modes of vibrations for a finite beam is demonstrated by considering a simply supported beam. The boundary conditions for a simply supported beam are according to Table 1 given as $w = 0$, $\partial\beta/\partial x = 0$ and $\partial^2 w/\partial x^2 = 0$ for $x = 0$ and L. The displacement w is given in equation (21) and the angular displacement β in equation (22). The six boundary conditions in combination with equation (23) give a system of equations, which can be written in matrix form as

$$\begin{bmatrix} 0 & 1 & 1 & e^{-\kappa_2 L} & 1 & e^{-\kappa_3 L} \\ \sin\kappa_1 L & \cos\kappa_1 L & e^{-\kappa_2 L} & 1 & e^{-\kappa_3 L} & 1 \\ 0 & X_2\kappa_1 & -X_3\kappa_2 & X_4\kappa_2 e^{-\kappa_2 L} & -X_5\kappa_3 & X_6\kappa_3 e^{-\kappa_3 L} \\ -X_1\kappa_1 \sin\kappa_1 L & X_2\kappa_1 \cos\kappa_1 L & -X_3\kappa_2 e^{-\kappa_2 L} & X_4\kappa_2 & -X_5\kappa_3 e^{-\kappa_3 L} & X_6\kappa_3 \\ 0 & -\kappa_1^2 & \kappa_1^2 & \kappa_2^2 e^{-\kappa_2 L} & \kappa_3^2 & \kappa_3^2 e^{-\kappa_3 L} \\ -\kappa_1^2 \sin\kappa_1 L & -\kappa_1^2 \cos\kappa_1 L & \kappa_2^2 e^{-\kappa_2 L} & \kappa_2^2 & \kappa_3^2 e^{-\kappa_3 L} & \kappa_3^2 \end{bmatrix} \begin{bmatrix} A_1 \\ A_2 \\ A_3 \\ A_4 \\ A_5 \\ A_6 \end{bmatrix} = 0. \tag{24}$$

The first line is obtained for $w = 0$ at $x = 0$ and the second at $x = L$. The third and fourth are for $\partial\beta/\partial x = 0$ first at $x = 0$ and then at $x = L$. The last two lines are obtained when $\partial^2 w/\partial x^2 = 0$ for $x = 0$ and L respectively. The eigenfrequencies are obtained as solutions to the determinant of the matrix being zero. For each solution or eigenfrequency, the relative ratio of the amplitudes are obtained from equation (24) by setting $A_1 = 1$. The amplitudes B_i are thereafter obtained from equation (23).

By using the method outlined above the first eight eigenfrequencies for beam A_y, described in Table 2, are predicted for the boundary conditions of the beam being free, clamped and simply supported. The resulting eigenfrequencies are listed in Table 3. For comparison, the corresponding eigenfrequencies using the Euler beam theory are also given in Table 3. For the Euler beam the bending stiffness is set to equal D_1 defined in equation (3).

The eigenfrequencies predicted from the Euler beam theory are always higher than the corresponding eigenfrequencies derived as described above; the reason being that shear and

TABLE 3

Predicted eigenfrequencies for beam A_y in vacuum; $L = 1{\cdot}2$ m

Eigenfrequency (Hz)	Free ends		Clamped ends		Simply supported ends	
	Euler	Sandw.	Euler	Sandw.	Euler	Sandw.
f_1	38	37	38	37	17	17
f_2	106	103	106	101	68	66
f_3	207	199	207	196	152	147
f_4	342	326	342	320	271	258
f_5	511	479	511	470	423	397
f_6	714	658	714	644	609	562
f_7	952	859	952	839	829	750
f_8	1222	1080	1222	1054	1083	960

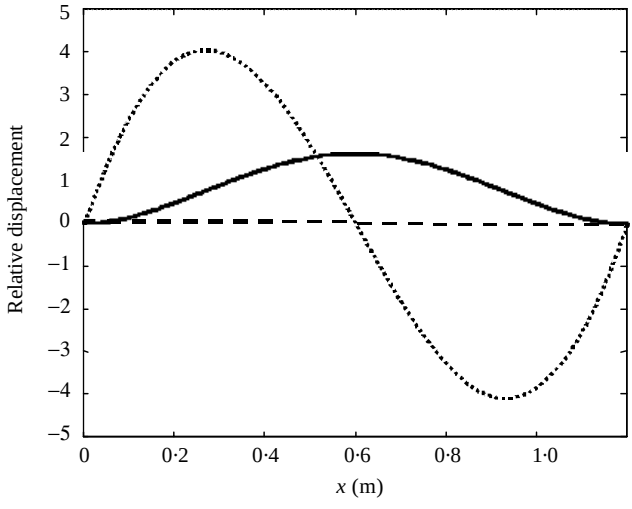

Figure 5. Relative displacement of beam A_y at $f_1 = 37$ Hz, clamped edges: —— w; ····· β; - - - - γ.

rotation are not included in the Euler beam model. The deviations between the results derived from the two models tend to increase for increasing frequencies. For the Euler beam, the eigenfrequencies for clamped and free boundaries are the same. This is not the case using the model presented in section 3. For a clamped beam, shear is induced at the boundaries thus rendering the beam more flexible as compared to a beam with free edges. The eigenfrequencies for a clamped beam are consequently lower than the corresponding eigenfrequencies for the same beam with free edges.

Plot of the displacement of the honeycomb beam at any of the eigenfrequencies shows the influence of shear and bending. The displacement w and the angular displacement β and γ are shown in Figure 5 for a clamped beam at the eigenfrequency f_1. The angular displacement γ caused by shear is negligible for the first mode. For mode 8 the influence of shear is substantial as seen in Figure 6.

For a beam with clamped boundaries, the effect of shear is very pronounced close to the edges. The angular displacement γ due to shear is zero at an edge and changes considerably over a very short distance close to the edge. This step-like behaviour is due to terms like $A_5 e^{-\kappa_3 x}$ where $\kappa_3 \gg 1$ in equation (21) defining the displacement.

The displacement w and angular displacements β and γ for mode 4, corresponding to 324 Hz for beam A_y with free edges, are shown in Figure 7.

The eigenfrequencies for a clamped and a free beam are according to the Euler theory identical. However, when shear is considered as in Table 3, there is a difference between the eigenfrequencies for the two conditions; the eigenfrequencies for the clamped boundaries being lower. This is due to the fact that shear in the beam is induced by the clamped boundaries. This is not the case for a beam with free edges as demonstrated in Figure 7. The apparent bending stiffness for the clamped beam is, therefore, somewhat lower than the corresponding bending stiffness for the same beam with free ends.

7. DYNAMIC PROPERTIES OF BEAM

In the previous section, the wave equation governing the displacement of a honeycomb beam was derived. Based on this differential equation wavenumbers, eigenfrequencies and

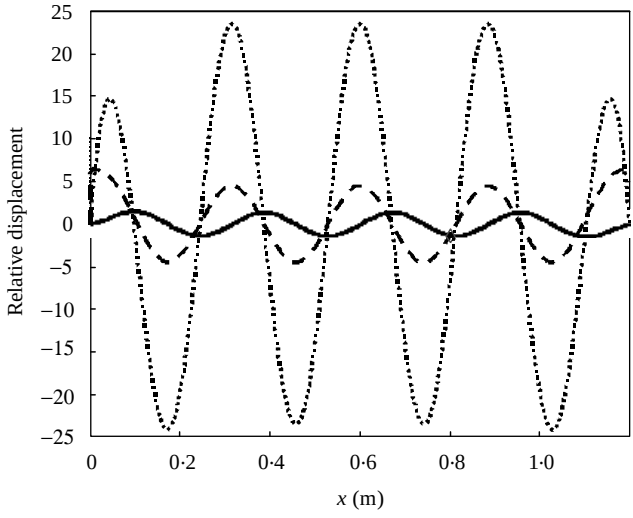

Figure 6. Relative displacement of beam A_y at $f_8 = 1054$ Hz, clamped edges: —— w; ····· β; - - - - γ.

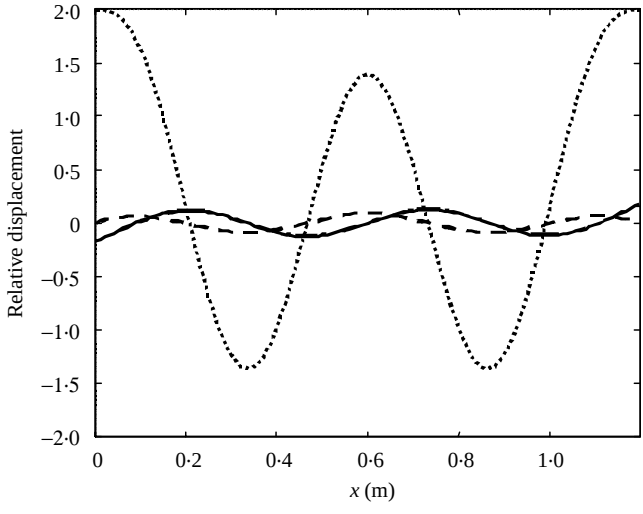

Figure 7. Relative displacement of beam A_y at $f_4 = 324$ Hz, clamped edges: —— w; ····· β; - - - - γ.

modes of vibration can be determined for different boundary conditions. For the response of a beam to be calculated, all the material parameters of the beam must be known. The dynamic properties of a composite beam are not always well defined. This is due to the fact that the elements of the assembled structure perform differently when bonded together as compared to when vibrating separately. However, the main dynamic properties of a composite beam can be determined from measurements of the first few eigenfrequencies when the structure is freely suspended.

Returning to equation (18), the wavenumber $k_x = \kappa_1$ for the first propagating wave can be written as $k_x^4 = \omega^2 \mu / D_x$ where D_x is the apparent bending stiffness of the structure. Consequently D_x can, as a first approximation, be defined as the bending stiffness of

a simple homogeneous beam which at a certain frequency has the same dynamic properties as the honeycomb structure. By inserting the definition of k_x in the wave equation (18), an equation in D_x is obtained. The resulting expression can generally be simplified whenever $D_1 \gg D_2$ and $\omega^2 I_\rho < G_e H$. For the structures discussed here, these assumptions hold for frequencies below 4 kHz as shown in reference [22]. The apparent bending stiffness D_x is, considering these approximations obtained as the solution to equation

$$\left(\frac{G_e H}{\mu^{1/2}\omega}\right)\left[\frac{D_x^{3/2}}{D_1} - D_x^{1/2}\right] + D_x - 2D_2 = 0. \tag{25}$$

In the low-frequency range, or as $\omega \to 0$, the first part of the equation dominates and so $D_x \to D_1$. The bending stiffness is consequently determined by pure bending of the beam. In the high-frequency range, when $\omega \to \infty$, $D_x \to 2D_2$. For high frequencies, the laminates are assumed to move in phase. In this frequency range, the bending stiffness for the entire beam is equal to the sum of the bending stiffness of the laminates. This agrees with the results discussed in the previous sections. For a beam with boundary conditions well defined, the bending stiffness can be determined by means of simple measurements. The apparent bending stiffness D_{xn} for mode n having the eigenfrequency f_n is for a beam, length L and mass per unit area μ, given by

$$D_{xn} = 4\pi^2 f_n^2 \mu L^4/\alpha_n^4 \quad \text{for } n = 1, 2, 3 \ldots, \tag{26}$$

where α_n is given in Table 4 for three boundary conditions.

For a simply supported beam $\alpha_n = n\pi$, measurements reveal the first few eigenfrequencies of the beam. The bending stiffness of a composite panel is strongly frequency dependent as given by equation (25). Equation (25) is written in a more general way as

$$\frac{A}{f} D_x^{3/2} - \frac{B}{f} D_x^{1/2} + D_x - C = 0, \tag{27}$$

where

$$A = \frac{G_e H}{\mu^{1/2} 2\pi D_1}, \quad B = \frac{G_e H}{\mu^{1/2} 2\pi}, \quad C = 2D_2. \tag{28}$$

For non-metallic materials, Young's modulus could exhibit slight frequency dependency as discussed in, for example, reference [4] and demonstrated in references [23, 24]. However within the frequency range of interest, here up to 4 kHz, the parameters D_1, D_2 and G_e in equation (28) are assumed to be constant for the structures investigated. Using the measured data, the parameters A, B and C can be determined by means of the least-square method. The quantity Q_1 is defined by

$$Q_1 = \sum_i \left(\frac{A}{f_i} D_{xi}^{3/2} - \frac{B}{f_i} D_{xi}^{1/2} + D_{xi} - C\right)^2 \tag{29}$$

TABLE 4

	n	1	2	3	4	5	$n > 5$
Free–free and clamped–clamped	α_n	4·73	7·85	11·00	14·14	17·28	$n\pi + \pi/2$
Free-clamped	α_n	1·88	4·69	7·85	11·0	14·14	$n\pi - \pi/2$

where D_{xi} is the measured bending stiffness at the frequency f_i for mode i. The parameters A, B and C are chosen to give the minimum of Q_1. The shear modulus G_e and the bending stiffnesses D_1 and D_2 can be determined, once the parameters A, B and C are calculated from equation (27).

Even if the inequalities $D_1 \gg D_2$ and $\omega^2 I_\rho < G_e H$ are not satisfied the equivalent bending stiffness can still be determined. The eigenfrequencies for the beam are first calculated as described in section 6. Thereafter, the equivalent bending stiffness is derived from equation (26) using the appropriate boundary condition.

The mass per unit area of a typical honeycomb panel used in an aircraft is often $< 3\ \mathrm{kg/m^2}$. Therefore, it is reasonable to consider the surrounding air to have an effect on the vibrations of such a panel. Theoretically, the apparent mass of an infinite panel when loaded by the surrounding air can be expressed as

$$\mu_0 = \mu + \mathrm{Re}\left(\frac{2\rho_0}{\sqrt{\kappa_p^2 - k^2}}\right), \tag{30}$$

which gives $\mu_0 = \mu$ for $\kappa_p < \mathrm{k}$. Here ρ_0 is the density of the surrounding fluid, κ_p is the wavenumber for propagating waves for the fluid-loaded panel, and is the solution to

$$\kappa_p = \kappa_0 \left[1 + \frac{2\rho_0}{\mu\sqrt{\kappa_p^2 - k^2}}\right]^{1/4}, \tag{31}$$

where κ_0 is the corresponding *in vacuo* wavenumber and k is the wavenumber in the fluid. Here the fluid is air and $k = 2\pi f/c$ with $c = 340$ m/s.

Results (30) and (31) give the mass load on an infinite plate.

8. MEASUREMENTS ON BEAMS

Measurements were performed on beams with different boundary conditions to verify the theories outlined in sections 3–7. The survey included beams with honeycomb as well as foam cores. The beams investigated also have different types of laminates. The material data for the tested structures are presented in Table 2.

The apparent bending stiffness was if possible determined for laminates, cores and the assembled structure. For certain types of lightweight honeycomb panels, the laminates are so thin as to make them almost completely limp with a tendency to curl up when not bonded to a core. For the types of laminates, the apparent bending stiffness is not readily defined. In order to determine the apparent bending stiffness of a beam, the beam was suspended by strings to simulate free–free boundary conditions. When suspended, the beams were excited with an impact hammer. The beam was excited perpendicular to the laminates and along the centreline of the beam to avoid twisting of the beam. The details are given in reference [22]. Due to the low mass of the material $\sim 3\ \mathrm{kg/m^2}$, the vibration measurements were made with a laser vibrometer to achieve non-contact measurements. The frequency response function was determined to give the eigenfrequencies for the beam. Based on the frequency response function the loss factor was also determined. The effect of the boundary conditions on the apparent bending stiffness were also investigated. Measurements were made on a beam with both ends free and with one end free and the other firmly mounted to simulate a clamped boundary.

For the sandwich beams tested, at least the first 10 modes and eigenfrequencies could be identified. In every case the length of each beam was approximately 1·2 m. The

measurement technique was tested on a beam with well-defined bending stiffness. The repeatability of the measurements was found satisfactory. The relative error when determining the apparent bending stiffness according to equation (29) is largest in the low-frequency range. For example, one set of four measurements of the third eigenfrequency f_3 of the lateral vibration of a beam gave the results 182·3, 184·3, 184·0 and 183·6 Hz. Measurements of the velocity on both laminates were recorded to verify that the laminates were moving in phase in the frequency range of interest. The details are discussed in reference [22].

Since honeycomb plates are predominantly anisotropic, measurements are performed on beams representing the two main inplane directions of the plate. For materials tested in two directions of the structure, the results are assigned a subscript x or y to indicate the orientations of the beam.

The dynamic performance of a beam is determined by expression (25) or from equation (27). The parameters A, B and C in equation (27) are functions of the shear modulus G_e and the bending stiffnesses D_1 and D_2. For each eigenfrequency f_n, the corresponding apparent bending stiffness D_{xn} is determined from equation (26). At least three sets of data, f_n and D_{xn}, determine the parameters A, B and C and thereby G_e, D_1 and D_2 as discussed in section 7.

The apparent frequency-dependent bending stiffness D_x for one type of honeycomb beam is shown in Figure 8. The predicted bending stiffness or rather the value D_x providing the best fit to the measured results as obtained from equation (29), the solid line, is determined from the first 12 eigenfrequencies of the freely suspended beam. For comparison, the effect of increased shear modulus, by a factor 10, is also indicated in the figure. In addition, the figure shows the effect of increasing the E-modulus of the laminates from 70 to 80 GPa.

The method to determine the dynamic parameters of a beam presented in section 7 can be somewhat improved. If equation (27) is used to determine the parameters A, B and C, the low-frequency measurements will dominate. The parameter A which depends on the static bending stiffness D_1 is therefore determined from equation (27). If instead the quantity to be minimized is defined as

$$Q_2 = \sum_i (AD_{xi}^{3/2} - BD_{xi}^{1/2} + f_i D_{xi} - f_i C)^2 \tag{32}$$

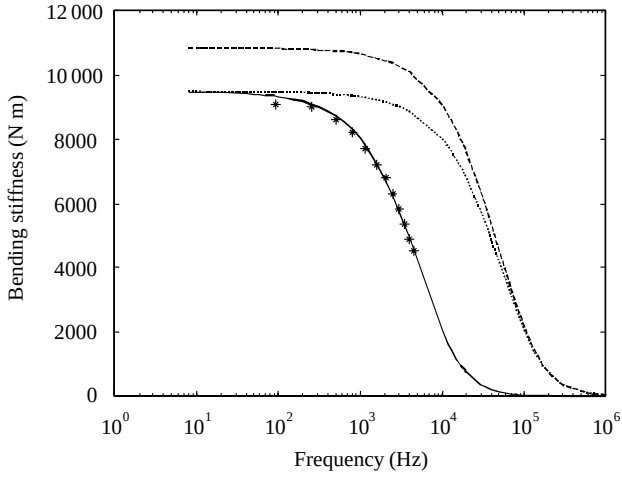

Figure 8. Predicted bending stiffness: ——, beam C_y; – · – · –, beam C_a, increased shear; – – – – beam C_b, increased bending stiffness of laminates; ✱✱✱, measured results, beam C_y.

the high-frequency response of the beam will dominate. When using A derived from equation (27), the parameter C is determined from equation (32) by setting $\partial Q_2/\partial B = 0$ and $\partial Q_2/\partial C = 0$. In the mid-frequency region, Q is written as

$$Q_3 = \sum_i \left(\frac{A}{\sqrt{f_i}} D_{xi}^{3/2} - \frac{B}{\sqrt{f_i}} D_{xi}^{1/2} + \sqrt{f_i} D_{xi} - \sqrt{f_i} C \right)^2, \tag{33}$$

where A and C are now known parameters. The parameter B is then determined by setting $\partial Q_3/\partial B = 0$.

In section 6, the first few eigenfrequencies are predicted for beams with different boundary conditions. In Table 5 some of these predictions are compared with measured results. The measurements were made on beam A_x when freely suspended. In addition, measurements are also made in such a way as to simulate a clamped boundary condition at one end of the beam with the other end free.

The corresponding bending stiffness is obtained from equation (26). The measured bending stiffness for the free–clamped beam is slightly lower than that for the free–free beam. This confirms the conclusion in section 6.

Figure 9 shows measured bending stiffnesses for two beams A_x and A_y, from the same panel with a Nomex core. Again, the beams represent two perpendicular directions. Not only the core, but also the laminates are orthotropic. The measured bending stiffnesses are different even in the high-frequency region, the reason being that the laminates are orthotropic.

The models derived are also tested on sandwich beams with foam cores. Two beams having the same laminates and the same core thickness were manufactured. In one case the core consisted of an aluminium honeycomb structure. For the other beam, the core material is foam with isotropic properties. In both cases the core thickness is 10 mm. The laminates are made of a 0.8 mm thick aluminium plate. The measured and predicted results are presented in Figure 10.

As seen from the figure, the differences in core shear give big differences in bending stiffness. For low and high frequencies, the values are the same for the two specimens due to the laminates being the same for both beams. It is interesting to note that the two different cores give the same stiffness, which means that the core material itself is of minor

TABLE 5

Eigenfrequencies, beam A_x

Measured				Calculated			
Free–free $L = 1{\cdot}2$ m		Free–clamped $L = 0{\cdot}963$ m		Free–free $L = 1{\cdot}2$ m		Free–clamped $L = 0{\cdot}963$ m	
f_n (Hz)	D (Nm)	f_n (Hz)	D (Nm)	f_n (Hz)	D (Nm)	f_n (Hz)	D (Nm)
46	937	11	942	46	943	11	887
127	914	70	896	126	907	68	846
243	869	191	856	243	873	187	822
393	831	362	804	391	829	355	772
568	782	576	745	567	779	564	715
764	725	821	678	764	726	807	655
983	678	1093	616	979	673	1076	597
1210	622	1389	561	1208	620	1364	541

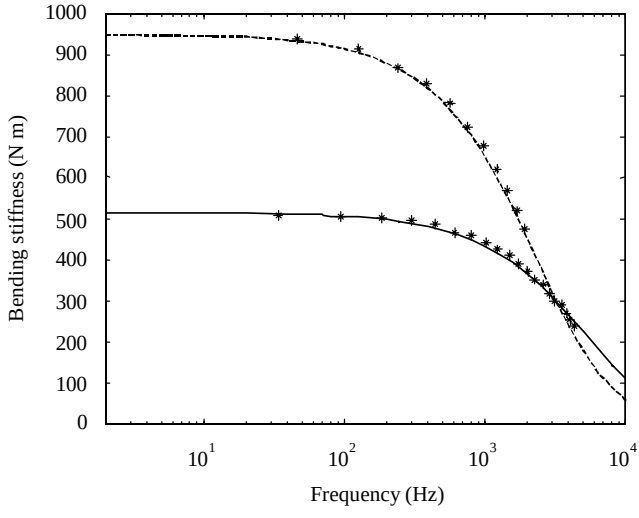

Figure 9. Bending stiffnesses for two beams A_x and A_y from the same panel with a honeycomb core. Calculations: —— D_x; – – – – D_y; ✱✱✱, measured results.

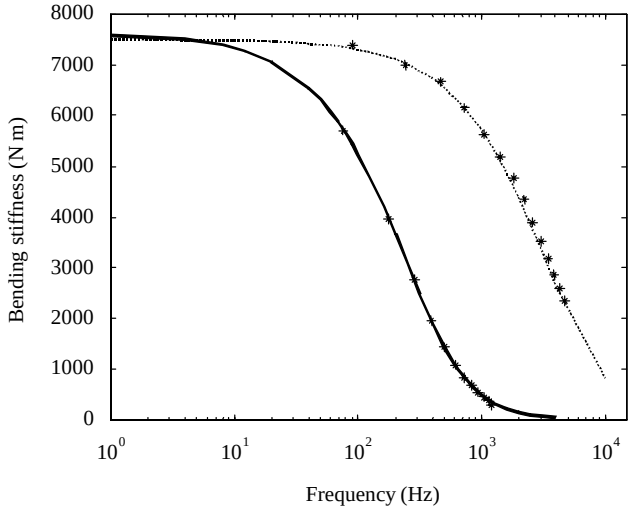

Figure 10. Bending stiffness of sandwich beams with Al laminates: ——, beam D foam core; ·····, beam E honeycomb core; ✱✱✱ measured results.

importance in the low-frequency region. In the mid-frequency region the bending stiffness for the beam with the honeycomb core is significantly higher than that for the beam with the foam core. This is due to the difference in shear stiffness between the cores.

In all the cases discussed, the apparent bending stiffness D_x approaches the bending stiffness $2D_2$ for increasing frequencies in accordance with result (25). If instead, the Timoshenko approximation is used for the entire beam, the measured data should according to reference [22] be fitted to a function of the form

$$D_{xi} + Vf_i\sqrt{D_{xi}} - W = 0, \tag{34}$$

where V and W are functions of the dynamic properties of the beam. Based on this expression, the parameters D_1, D_2 and G_e cannot be determined from simple beam measurements. Further, the apparent bending stiffness D_x would according to equation (34) decay as $1/f^2$ in the high-frequency range instead of approaching the limit $2D_2$.

9. FLUID LOADING

For lightweight structures, the surrounding air can be assumed to have an effect on the vibrations of the material for low frequencies.

The fluid loading on a panel is equivalent to an added mass to the structure in the low-frequency region. The added mass due to the fluid tends to decrease the eigenfrequencies of the panel as compared to the *in vacuo* situation. In order to verify this, the first few eigenfrequencies of a beam were measured inside a vacuum chamber. Two measurement series were made; the first *in vacuo* and the second under normal pressure with the chamber open or rather with the end section removed. In both cases, the beam was suspended by strings inside the chamber to simulate free–free boundary conditions. The beam was excited by an electro-dynamic shaker. The response of the beam was measured by means of a laser vibrometer using a window in the vacuum chamber as shown in Figure 11. The added mass effect can be calculated from equation (30), the bending stiffness of the beam being the same in both the cases. The total mass per unit area of the beam is shown in Figure 12. This total mass is the sum of the actual mass of the beam and the added mass due to the fluid loading. The actual mass per unit area is 2·64 kg/m^2. The dashed line in the figure represents the predicted total mass per unit area as given by equation (30).

The agreement between the predicted and measured results is satisfactory despite the fact that the predicted result is based on a model valid only for infinite plates whereas the measurements were made on finite beams. It can be concluded from Figure 12 that the added mass effect is of the order 30% of the actual mass of the beam in the low-frequency region. The maximum just above 1 kHz is due to the coincidence effect. This maximum would be smoothed to give better agreement with measurement at around coincidence if losses were included.

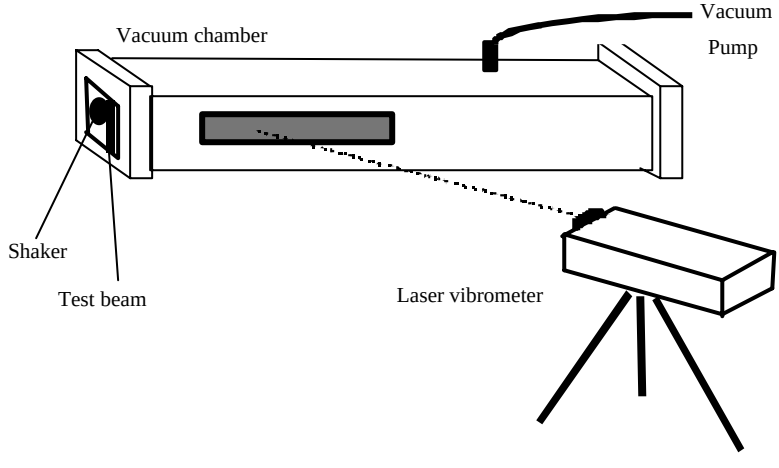

Figure 11. Measurements in vacuum chamber.

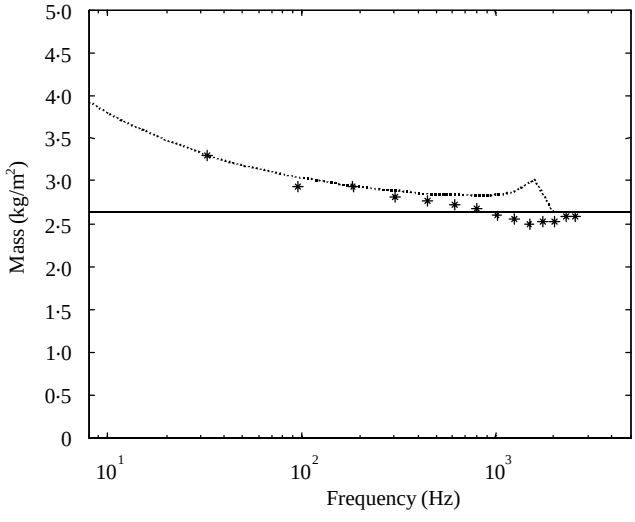

Figure 12. Total mass of beam A_y: ——, *in vacuo*; ·····, with fluid loading; ✱✱✱, measured results.

10. BENDING OF HONEYCOMB PLATES

An expression defining pure bending of an orthotropic plate is as discussed in references [2, 3] given by

$$D_{11}\frac{\partial^4 w}{\partial x^4} + 2(D_{12} + 2D_{66})\frac{\partial^4 w}{\partial x^2 \partial y^2} + D_{22}\frac{\partial^4 w}{\partial y^4} + \mu\frac{\partial^2 w}{\partial t^2} = 0. \tag{35}$$

The bending stiffnesses D_{ij} are defined as

$$D_{11} = \frac{D_x}{1 - v_{xy}v_{yx}}, \quad D_{22} = \frac{D_y}{1 - v_{xy}v_{yx}}, \quad D_{12} = \frac{v_{yx}D_x}{1 - v_{xy}v_{yx}} = \frac{v_{xy}D_y}{1 - v_{xy}v_{yx}}, \quad 2D_{66} = D_{xy}. \tag{36}$$

In certain cases, as discussed in reference [25], the torsional rigidity $(D_{12} + 2D_{66})$ can be replaced by $\sqrt{D_x D_y}$. This substitution can be made whenever the shear modulus G_{xy} is approximated by $\sqrt{E_x E_y}/[2(1 + \sqrt{v_{xy}v_{yx}})]$. In reference [12], the ratio $\alpha = (D_{12} + 2D_{66})/\sqrt{D_x D_y}$ is discussed for some typical honeycomb structures. It is demonstrated that the parameter α can be as low as 0·06. The bending of such a plate is consequently dominated by the bending stiffness in the x and y directions. It is therefore reasonable to assume that the bending of honeycomb plates can be approximated by the expression

$$\left[\frac{1}{1 - v_{xy}v_{yx}}\right]\left[D_x\frac{\partial^4 w}{\partial x^4} + 2\alpha\sqrt{D_x D_y}\,\frac{\partial^4 w}{\partial x^2 \partial y^2} + D_y\frac{\partial^4 w}{\partial y^4}\right] + \mu\frac{\partial^2 w}{\partial t^2} = 0, \tag{37}$$

where the parameters D_x and D_y represent the apparent bending stiffness of beam elements in the x and y directions of the plate. In general $(1 - v_{xy}v_{yx})$ can, as a first approximation, be set to equal unity. This is equivalent to saying that the test beams used are modelled as narrow plates. The eigenfrequencies f_{mn} for a simply supported and rectangular plate satisfying equations (37) are given by

$$f_{mn} = \pi^2[D_x(m/L_x)^4 + 2\alpha\sqrt{D_x D_y}(m/L_x)^2(n/L_y)^2 + D_y(n/L_y)^4]^{1/2}/\sqrt{4\mu}, \tag{38}$$

where m and n are integers and L_x and L_y are the dimensions of the rectangular plate along the x- and y- axis. The parameters D_x, D_y and μ are frequency dependent. Equation (38) is solved by iteration.

For a plate with free or clamped edges and satisfying equation (35), the eigenfrequencies can be estimated by means of the Rayleigh–Ritz method [4]. By using simple beam functions satisfying the proper boundary conditions, the eigenfrequencies f_{mn} for a rectangular plate with free edges are according to Blevins [26] given by

$$f_{mn} = \frac{\pi}{2\sqrt{\mu}} \sqrt{\left(D_x \left(\frac{G_m}{L_x}\right)^4 + D_y \left(\frac{G_n}{L_y}\right)^4 + \frac{2J_m J_n + 2v(H_m H_n - J_m J_n)}{(L_x L_y)^2} \alpha \sqrt{D_x D_y} \right)}, \quad (39)$$

where

$$G_m = 0, \quad H_m = 0, \quad J_m = 0 \quad \text{for } m = 0,$$

$$G_m = 0, \quad H_m = 0, \quad J_m = 1{\cdot}216 \quad \text{for } m = 1,$$

$$G_m = 1{\cdot}506, \quad H_m = 1{\cdot}248, \quad J_m = 5{\cdot}017 \quad \text{for } m = 2,$$

$$G_m = m - \frac{1}{2}, \quad H_m = G_m \left(1 - \frac{2}{\pi G_m}\right), \quad J_m = G_m^2 \left(1 + \frac{6}{\pi G_m}\right) \quad \text{for } m > 2. \quad (40)$$

As before D_x, D_y and μ are frequency dependent and should be evaluated at $f = f_{mn}$.

The first few eigenfrequencies for a plate were measured in the same way as for the beams, described in section 8. The plate was suspended by strings to simulate free boundary conditions. The plate was hanging vertically. The measurements were repeated with the plate resting on a soft and resilient layer, to ensure that the recorded eigenfrequencies were not influenced by the mounting. The dimensions of the plate were $L_x = 1{\cdot}2167$ m and $L_y = 0{\cdot}429$ m. The material and geometrical parameters for the plate or structure A or rather A_x and A_y are given in Table 2. The bending stiffnesses D_x and D_y are shown in Figure 9.

The eigenfrequencies for the plate A with free edges can now be obtained from expression (39). The parameters D_x, D_y and μ are all frequency dependent. The parameter α is adjusted to give a good agreement between the predicted and measured eigenfrequency for mode (1,1). The parameter α is set to equal 0·3. If all the material and geometrical parameters are well defined, the quantities D_x, D_y and μ can be calculated as functions of frequency. The first few measured and predicted eigenfrequencies for plate A are compared in Figure 13.

11. CONCLUSION

Some of the dynamic properties of symmetric sandwich beams with honeycomb cores can be derived using Hamilton's principle. The results could be extended to also include asymmetric structures. The laminates can be considered as being thin plates. Shear effects in the core as well as rotation are included. However, for most types of lightweight structures the shear rather than the rotational effects tend to dominate.

Based on Hamilton's principle, a sixth order differential equation governing the displacement of the beam is derived. For free vibrations of the beam, the shear angle is found to satisfy the same differential equation as the displacement. In the very low frequency range, the lateral motion of a sandwich beam is determined by pure bending of

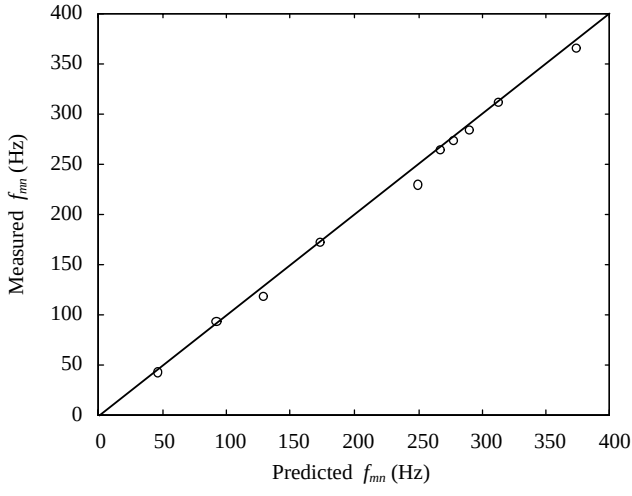

Figure 13. Measured and predicted eigenfrequencies for plate A, $1{\cdot}22 \times 0{\cdot}43$ m^2.

the entire construction. The corresponding limit in the high-frequency range is given by the flexural motion of the seemingly uncoupled laminates. Consequently the apparent bending stiffness of the beam is strongly dependent on frequency and is to a certain extent, determined by the properties of the laminates, decreasing with increasing frequencies. If, however, the bending of a sandwich beam is described by means of the Timoshenko model the apparent bending stiffness is found to decrease monotonously.

The boundary conditions for free, clamped and simply supported beams are also obtained using Hamilton's principle. At each edge three boundary conditions must be satisfied. The apparent bending stiffness of a sandwich beam is found to decrease as the boundary conditions are constrained. This is due to shear effects being induced. This effect is enhanced by increasing the thickness of the core.

The effective shear stiffness of the core, the bending stiffness of laminates as well as the bending stiffness of the entire beam can be determined based on simple measurements on the assembled beam. The models developed can also be used to describe some of the dynamic properties of sandwich beams with foam cores. The added mass effect due to a fluid loading on a lightweight structure can in the low-frequency region be sufficiently well described by means of a model derived for infinite structures. The fluid loading can be considerable or of the order 30% of the weight of lightweight panels in the low-frequency range.

The eigenfrequencies of orthotropic plates can be estimated fairly accurately based on measurements on beams representing the two main axes of the plate.

REFERENCES

1. N. J. HOFF 1950 *NACA TN* 2225. Bending and buckling of rectangular sandwich plates.
2. D. ZENKERT 1997 *An Introduction to Sandwich Construction*. London: Chameleon Press Ltd.
3. J. WHITNEY 1987 *Structural Analysis of Laminated Anisotropic plates*. Lancaster, Basel: Technomic Publishing Company.
4. Y. C. FUNG 1965 *Foundations of Solid Mechanics*. Englewood Cliffs, NJ: Prentice-Hall, Inc.
5. R. D. MINDLIN 1951 *Journal of Applied Mechanics* **18**, 31–38. Influence of rotatory inertia and shear on flexural motions of isotropic, elastic plates.

6. G. KURTZE and B. WATTERS 1959 *Journal of Acoustical Society of America* **31**, 739–748. New wall design for high transmission loss or high damping.
7. C. L. DYM and M. A. LANG 1974 *Journal of Acoustical Society of America* **56**, 1523–1532. Transmission of sound through sandwich panels.
8. A. C. NILSSON 1990 *Journal of Sound and Vibration* **138**, 73–94. Wave propagation in and sound transmission through sandwich plates.
9. S. SANDER 1998 *ICA*-16, *Seattle*, *Washington*, *U.S.A.* Dynamic and acoustic properties of beams of composite material.
10. J. L. GUYADER and C. LESUEUR 1977 *Journal of Sound and Vibrations* **58**, 51–68. Acoustic transmission through orthotropic multilayered plates. Part I: plate vibration modes.
11. C. T. SUN and J. M. WHITNEY 1973 *American Institute of Aeronautics and Astronautics Journal* **11**, 178–183. On theories for the dynamic response of laminated plates.
12. K. RENJI, P. S. NAIR and S. NARAYANAN 1996 *Journal of Sound and Vibration* **195**, 687–699. Modal density of composite honeycomb sandwich panels.
13. K. M. LIEW 1996 *Journal of Sound and Vibrations* **198**, 343–360. Solving the vibration of thick symmetric laminates by Reissner/Mindlin plate theory and P-Ritz method.
14. Y. XIANG, K. M. LIEW and S. KITIPORNACHAI 1997 *Journal of Sound and Vibration* **204**, 1–16. Vibration analysis of rectangular Mindlin plates resting on elastic edge supports.
15. M. R. MAHERI and R. D. ADAMS 1998 *Journal of Sound and Vibration* **209**, 419–442. On the flexural vibration of Timoshenko beams and the applicability of the analysis to a sandwich configuration.
16. T. SAITO, R. D. PARBERY, S. OKUND and S. KAWANI 1997 *Journal of Sound and Vibration* **208**, 271–287. Parameter identification for aluminium honeycomb sandwich panels based on orthotropic Timoshenko beam theory.
17. C. C. CHAO and Y. C. CHERN 2000 *Journal of Sound and Vibration* **230**, 985–1007. Comparison of natural frequencies of laminates by 3-D theory.
18. G. SHI and K. Y. LAM 1999 *Journal of Sound and Vibration* **219**, 707–721. Finite element vibration analysis of composite beams based on higher-order beam theory.
19. P. R. CUNNINGHAM, R. G. WHITE and G. S. AGLIETTI 2000 *Journal of Sound and Vibration* **230**, 617–648. The effects of various design parameters on the free vibration of doubly curved composite sandwich beams.
20. K. M. LIEW, L. JIANG, M. K. LIM and S. C. LOW 1995 *Computers and Structures* **55**, 191–203. Numerical evaluation of frequency responses for delaminated honeycomb structures.
21. S. T. TIMOSHENKO 1978 *Strength of Materials*. New York: D. Van Norstrand Company, 3rd edition.
22. E. NILSSON 2000 *TRITA-FKT* 2000:30, *Department of Vehicle Engineering*, *KTH*, *Sweden*. Some dynamic properties of honeycomb structures.
23. K. DOVSTAM 1998 *Dr Tech. Thesis*, *Department of Solid Mechanics*, *KTH*, *Stockholm*, *Sweden*. On material damping modelling and modal analysis in structural dynamics.
24. L. KARI 1998 *Dr. Tech. Thesis*, *Report* 98-02, *MWL*, *Department of Vehicle Engineering*, *KTH*, *Stockholm*, *Sweden*. Structure–borne sound properties of vibration isolators.
25. R. SZILARD 1974 *Theory and Analysis of Plates*. Englewood Cliffs, NJ: Prentice-Hall, Inc.
26. R. D. BLEVINS 1984 *Formulas for Natural Frequency and Mode Shape*. Malabar, FL: Krieger Publishing Company.